Pharmacological Research 74 (2013) 34–44

Contents lists available at SciVerse ScienceDirect

Pharmacological Research

journal homepage: www.elsevier.com/locate/yphrs

Hydrogen sulfide restores a normal morphological phenotype in Werner syndrome fibroblasts, attenuates oxidative damage and modulates mTOR pathway

F. Talaei*, V.M. van Praag, R.H. Henning

Department of Clinical Pharmacology, University Medical Center Groningen, University of Groningen, The Netherlands

ARTICLE INFO

Article history:
Received 15 February 2013
Received in revised form 29 April 2013
Accepted 30 April 2013

Keywords:
Werner protein
Aging
Progeria
Proteostasis
mTOR
Autophagy
NaHS

ABSTRACT

Werner syndrome (WS) protein is involved in DNA repair and its truncation causes Werner syndrome, an autosomal recessive genetic disorder with a premature aging phenotype. WRN protein mutation is currently known as the primary cause of WS. In cultured WS fibroblasts, we found an increase in cytosolic aggregates and hypothesized that the phenotype is indirectly related to an excess activation of the mTOR (mammalian target of rapamycin) pathway, leading to the formation of protein aggregates in the cytosol with increasing levels of oxidative stress.

As we found that the expression levels of the two main H_2S producing enzymes, cystathionine β synthase and cystathionine γ lyase, were lower in WS cells compared to normal, we investigated the effect of administration of H_2S as NaHS (50 μM). NaHS treatment blocked mTOR activity, abrogated protein aggregation and normalized the phenotype of WS cells. Similar results were obtained by treatment with the mTOR inhibitor rapamycin.

This is the first report suggesting that hydrogen sulfide administered as NaHS restores proteostasis and cellular morphological phenotype of WS cells and hints to the importance of transsulfuration pathway in WS.

1. Introduction

Werner syndrome (WS) is a prototype of segmental post-puberty progeria characterized by the accelerated appearance of common aging-related pathologies including alopecia, ischemic heart disease, osteoporosis, ocular cataract, type II diabetes mellitus, hypogonadism [1] and mesenchymal neoplasms, particularly sarcomas [2]. WS is caused by the mutation of Werner protein, a member of the RecQ family of DNA helicases [3]. The resulting truncation of WRN protein leads to defects in important DNA metabolic pathways, such as replication, recombination and maintenance of telomeres [4,5]. Depletion of WRN protein in normal fibroblasts reduces cell survival and increases senescence associated β-galactosidase activity [6], is highly growth suppressive and sensitizes cells to DNA damage [7] to a level comparable to primary WS fibroblasts. It has been demonstrated that WRN protein knockdown (e.g. via shRNA) in human fibroblasts causes growth suppression and sensitization to DNA damage [7]. The genome instability of WS cells depends on WRN protein expression, because in vitro expression of normal WRN protein or telomerase in WS cells is sufficient to partially protect them from the accumulation of chromosomal aberrations and genome instability [8]. Mutational inactivation of the WRN gene causes Werner syndrome, an autosomal recessive disease characterized by premature aging, elevated genomic instability and increased incidence of cancer. The genetic data indicate that the delayed manifestation of the complex pleiotropic of WRN deficiency might relate to telomere shortening [8], although there is still controversy over the exact role of telomeres in WS. Further, despite the extensive changes in fibroblasts depleted of WRN protein, WRN protein knockout mice show no sign of accelerated aging, although their cellular proliferative capacity is reduced [9,10]. Also, WRN protein knockout does not increase the sensitivity of mouse embryonic fibroblast to camptothecin induced cell death [10]. Thus, although the lack of WRN is the cause of the accelerated aging in WS, the absence of a clear phenotype in WRN knockout mice indicates that a different mechanism is required in mice to recapitulate human WS. Perhaps, the absence of WRN protein embodies only one factor involved in the aging phenotype observed in WS and additional factors might be part of the disease mechanism.

We observed a morphological difference between WS fibroblasts and normal fibroblasts and hypothesized this difference to arise from protein aggregation in response to environmental stress

* Corresponding author at: Department of Clinical Pharmacology (FB20), University Medical Center Groningen, PO Box 196, 9700 AD Groningen, The Netherlands. Tel.: +31 50 3632810; fax: +31 50 3632812.
E-mail addresses: Talaei@irimc.org, talaeifate@gmail.com (F. Talaei).

1043-6618/$ – see front matter © 2013 Elsevier Ltd. All rights reserved.
http://dx.doi.org/10.1016/j.phrs.2013.04.011

and genetic mutations [11]. Protein aggregate formation affects cellular function and has been implicated in various aging related disorders [12] and complications as reviewed by Talaei [13]. Indeed, cells from WS patients show high levels of oxidatively modified proteins [14], which might contribute to an accumulation of reactive oxygen species (ROS) [15,16], in turn likely negatively affecting DNA stability [17] and possibly contributing to aggregation of oxidized proteins [18]. Moreover, while in normal cells oxidative damage of DNA leads to inhibition of proliferation, this process seems impaired in WS [19]. This in turn potentially promotes DNA double-strand breaks [20] and genome instability, which is in part due to defect in telomere maintenance [8]. It has been suggested that genome instability in WS cells depends directly on telomere dysfunction, linking chromosome end maintenance to chromosomal aberrations in this disease [8]. This might in part also be related to the observation that cells in WS cultures usually exhibit premature senescence by an apparently irreversible exit from the cell cycle at a faster rate than normal cells do [21]. Also, extracellular matrix (ECM) protein components are affected by senescence, acquiring insoluble properties [22]. Thus, certain clinical manifestations of WS such as fibrosis, cataract, scleroderma and osteoporosis may be dependent on the expression of aberrant ECM components such as hyaluronate, fibronectin and collagens [23].

According to our observations in WS fibroblast cells, we hypothesized that administration of H_2S might constitute an effective therapy against cellular damage in WS cells. First, H_2S displays profound antioxidant and cytoprotective properties, protecting against ROS [24,25]. Secondly, in kidney cells, H_2S inhibits the activity of mammalian target of rapamycin (mTOR) [26], a major pathway controlling protein translation via its downstream targets S6 kinase and 4EBP1 [27,28]. Thus, we explored the effects of H_2S in WS skin fibroblasts compared to normal skin fibroblasts by studying its effect on protein aggregation, mTOR and downstream targets and autophagy. Rapamycin treated cells were used to examine the effects of mTOR inhibition. Also, we studied the levels of enzymes involved in the endogenous production of H_2S, cystathionine β synthase (CBS) and cystathionine γ lyase (CSE) in WS cells.

2. Materials and methods

2.1. Cell lines

WS skin fibroblast cell lines; AG11395 (male, 60 years old, SV40 transformed) and AG12795 (male, 19 years old, non-transformed) were selected for the experiments and purchased from Coriell institute cell repository (NJ, USA). Normal skin fibroblast cells; GM00637 (female 18 years Corriell NIGMS human genetic cell collection, SV40 transformed (NJ, USA)) and PCS-201-012 (American type culture collection, VA, USA), from healthy adult individuals were used as reference. According to the trypan blue exclusion assay, the different cell lines used at the time of experiments had similar population doubling time of 22 ± 2.3 h, indicating similar rates of cell growth in culture, even though unfortunately we have to record of PDL (population doubling level of these cell lines). Experiments with untreated and treated WS cells were performed in every single batch of cells. Cells were kept at 37 °C with 5% CO_2 in Dulbecco Modified Eagles Medium with 2 mM L-glutamine and 10% fetal bovine serum.

2.2. Cell treatment and assessment of intracellular proteins

To study the pharmacological effects of NaHS and rapamycin on cells, semiconfluent (50%) cultures at the above indicated doubling time were treated for 1 week on daily basis with either freshly dissolved NaHS (50 μM) or rapamycin (50 nM used only on AG11395 WS cells) in medium. Cells with different treatments and controls were cultured at low density and photographed by phase contrast microscopy. To analyze the properties of intracellular proteins, the SDS–urea resistant protein fraction was determined. Werner cells of an exponentially growing culture were harvested by centrifugation at $1400 \times g$ for 5 min at 4 °C and resuspended in 300 μl of lysis buffer (50 mM Tris pH 7.5, 100 mM EDTA, 10 mM KCl, 1 mM dithiothreitol, 1% Triton, 10 μg/ml leupeptin, 10 μg/ml pepstatin, 1 μg/ml aprotinin, and 1 mM phenylmethylsulfonyl fluoride), lysed on ice for 1 h, and disrupted by 4 min of vortexing. Cell aggregates were removed by centrifugation at $1400 \times g$ for 1 min.

Ultracentrifugation of 200 μl of extract at $350{,}000 \times g$ at 4 °C for 1 h was used to separate soluble and insoluble proteins. Pellets were washed twice with phosphate-buffered saline and resuspended in 200 μl of formic acid at 37 °C for 1 h. Protein content of the supernatant and solubilized pellet fraction was analyzed by Bradford assay. Sirius red dye was used to quantify the amount of collagen in supernatant medium obtained from treated WS and normal cells 24 h after the last treatment and compared to collagen present in supernatant from control cells. To prepare Sirius red dye solution, 0.2 g Sirius Red was added to 200 ml of saturated aqueous solution of picric acid. One milliliter of the dye solution was added to each 5 ml of cell supernatant, mixed gently at room temperature for 30 min and centrifuged at $10{,}000 \times g$ for 5 min to pellet the collagen. The supernatant was carefully removed without disturbing the pellet. One milliliter of 0.1 M HCl was added to each tube to remove unbound dye. The samples were again centrifuged at $10{,}000 \times g$ for 5 min to pellet the collagen. One milliliter 0.5 M NaOH was added to each tube and vortexed vigorously to release the bound dye. 100 μl of each solution was transferred to a 96 well plate and the absorption was read at 540 nm (500–550 nm). Collagen stock solution (2 mg/ml) was prepared by adding 5 ml of 0.5 M sterile acetic acid to 10 mg lyophilized powder (Type I Collagen – acid soluble (Sigma C-3511)). A standard curve was constructed using different concentration of collagen [29].

2.3. Initiation of oxidative stress

The effect of daily NaHS and rapamycin administration was tested in WS and normal fibroblasts subjected to H_2O_2 oxidative stress. One week treated WS cells were washed with PBS and the medium was renewed without any treatment, incubated for 24 h and subsequently exposed to 100 μM H_2O_2 for 30 min. Cells were studied 24 h after exposure. To assess the level of cell apoptosis in each cell group, cell viability was measured by MTS assay (Promega) according to the manufacturer's instructions.

2.4. Assessment of intracellular thiol groups

After 1 week of treatment with NaHS and rapamycin, total levels of cellular sulfhydryl groups (—SH groups) based on the reduction of 5,5 dithiobis-2-nitrobenzoic acid (DTNB, Sigma). Cells were measured 24 h after exposure to H_2O_2 stress and compared to non-exposed control. Cells were lysed in 10 mM Tris-buffer 1% Triton X-100 (Sigma), followed by centrifugation at $7000 \times g$ for 10 min. The supernatant was incubated with phosphate buffer containing DTNB at room temperature for 60 min. The quantification was conducted at 412 nm using a microplate reader.

2.5. ROS formation

Intracellular reactive oxygen species (ROS) generation by cells was measured using the fluorogenic probe CM-H2-DCFDA (2,7 dichlorofluorescein diacetate, Invitrogen). Cells were cultured in black 96-well plates (Nunc). 24 h later confluent cells were exposed to 100 μM H_2O_2 for 30 min to elicit ROS response in cells. The

medium was then discarded and cells were loaded with 5 μM of CM-HDCFDA in PBS for 30 min at 37 °C. Serial measurement in a fluorescence 96-well plate reader at 37 °C was performed. The formation of the fluorescent probe DCF was monitored at excitation wavelength 488 nm (bandwidth 5 nm), and emission wavelength 525 nm (bandwidth 20 nm). Substrate autofluorescence was subtracted.

2.6. Caspase 3/7 activity assessment

To assess apoptosis, caspase 3/7 activity assay was performed. Cells were cultured in transparent 96 well plates and left at 37 °C for 24 h, treated with 100 μM H_2O_2 for 30 min, washed with normal medium and replaced with FCS supplemented medium without antibiotics and left to proliferate for 24 h. Caspase substrate (50 μl, Promega Apo-ONE) was added to each well. The plates were shaken for 3 h and fluorescence was read at an excitation of 499 nm and emission of 521 nm.

2.7. Antibody staining and Western blotting

Lamin A/C antibody (Santa Cruz, sc-6215) was used to assess nuclear morphology in fixed cells. Cells were cultured at 50% confluence on glass coverslips, fixed by acetone (100%) for 10 min and rehydrated in alcohol 70% for 10 min. The coverslips were washed with PBS three times for 5 min each. Then, cells were incubated with the appropriate antibody for 1 h. The slides were then washed in PBS thrice and incubated with 1% secondary antibody in PBS containing 1% BSA for 1 h and again washed in PBS thrice. Dako AEC + High sensitivity substrate chromogen (K3461) was used to visualize the antibody stain. To demonstrate the localization of this protein images were captured using a Nikon 50 light microscope with a Paxcam camera.

Western blot analysis was conducted to evaluate the expression of fibronectin (Santa Cruz antibody, sc-6952), CBS (Santa Cruz antibody, sc-46830) and CSE (Santa Cruz antibody, sc-131905). To evaluate the mTOR pathway, the expression of (phospho)proteins was quantified by Western blot analysis. The mTOR phosphorylation was analyzed by rabbit Anti-p-mTOR (ser 2448) (Millipore 15-105). Antibodies to proteins associated with the mTOR pathway were from Cell Signaling and included mTOR (7C10), pAkt (s473; D9E) and pS6 ribosomal protein S235/236 (D57.2.2E).

Cell samples were washed with PBS and lysed in 120 μl RIPA buffer (1% Igepal ca-630, 1% SDS, 5 mg/ml sodium deoxycholate, 1 mM sodium orthovanadate, 40 μg/ml PMSF, 100 μg/ml benzamidine, 500 ng/ml pepstatin A, 500 ng/ml leupeptine and 500 ng/ml aprotinin in PBS) [30]. Loading buffer (20 μl) was added to 50 μg of cell protein and ran at 100 V for 70 min. Proteins were transferred to a nitrocellulose membrane and detected by West Pico Chemiluminescent Substrate (supersignal), photographed and analyzed with genetool software (version 3.08, SynGene, UK). Protein expression was corrected over β-actin as an internal reference.

2.8. Senescence-associated β-galactosidase (SABG) activity

To evaluate the level of senescence in cells SABG staining was performed. Cells (SV40 nontransfected cells) were treated with NaHS or rapamycin on daily basis or left untreated as controls for one week. The final treatment dose was administered 2 h before the induction of premature senescence, accomplished by washing cells with PBS and the administration of 100 μM H_2O_2 for 30 min in culture medium. Subsequently, cells were washed with PBS and incubated in fresh culture medium at 37 °C with 5% CO_2 for 24 h before staining. Then, cells were washed twice in PBS, fixed in 2% formaldehyde and 0.2% glutaraldehyde for 5 min at room temperature, washed twice, and stained with fresh SABG staining solution (1 mg/ml of 5-bromo-4-chloro-3-indolyl-D-galactoside, 40 mmol/L of citric acid/sodium phosphate dibasic, pH 6.0, 150 mmol/L NaCl, 2 mmol/L of $MgCl_2$, 5 mmol/L of $K_3Fe[CN]_6$, and 5 mmol/L of $K_4Fe[CN]_6$) for 18 h at 37 °C without CO_2. Two hundred cells were examined at 100× magnification using a phase contrast microscope and the percentage of positively stained cells was determined.

2.9. Nuclei contour ratio

To determine nuclei roundness, nuclei contour ratios were computed. We measured 40–70 randomly selected cell nuclei per cell line and calculated the contour ratio ($4\pi \times \text{area/perimeter}^2$). The contour ratio for a circle is 1. As the cell nuclei become less round, this ratio approaches 0. To calculate the perimeter length and area, we traced the outline of cell envelop with a closed loop drawing tool using imageJ and by using images captured from cells prepared for immunohistochemistry.

2.10. Statistics

Data are presented as mean ± SD. Statistical data analyses were either performed using a One-way ANOVA ($P < 0.05$) with Tukey post hoc testing or a student's *t*-test (GraphPad Prism version 5.00 for Windows, GraphPad Software, San Diego CA, USA), unless indicated otherwise.

3. Results and discussion

3.1. Aggregates in WS cells, autophagy and annihilation by NaHS

We studied protein aggregation and the nature of protein aggregates in different samples. The data from the experiments represent WS cell lines and Normal cell lines (WS: AG11395 and AG12795, Normal: GM00637 and PCS-201-012) unless indicated otherwise. Upon light microscopic examination, normal fibroblast visibly shows little presence of vesicular shaped aggregates per cell (Fig. 1A panels 1 and 2) compared to WS cells (Fig. 1A, panels 3 and 6). Treatment of WS fibroblasts with both NaHS (Fig. 1A, panels 4 and 7) and rapamycin (Fig. 1A, panels 5 and 8) for 1 week decreased the vesicular structures inside the cells and WS fibroblasts appeared similar to normal cells. We also observed different cell morphology with different treatments. WS cells displayed a larger size and rounder morphology compared to normal or treated cells, which were smaller and more spindle shaped, likely representing a less active state of these fibroblasts. Thus, NaHS and rapamycin restored the light microscopic phenotype of WS cells.

The nature of cytosolic proteins in WS cells was investigated by measuring the urea-insoluble portion of proteins compared to the soluble portion. In WS fibroblasts, insoluble proteins made up for 50 ± 5% of protein content, as opposed to only 15 ± 5% in normal cells (Fig. 1B). Treatment of WS cells with NaHS and rapamycin fully normalized the levels of insoluble proteins.

To further characterize the protein production in WS fibroblasts, cellular collagen release into the medium was measured in WS cells compared to normal fibroblasts (Fig. 1C). WS fibroblasts produced twice the amount of collagen compared to normal fibroblasts. NaHS treatment significantly reduced the collagen amount produced by WS cells, almost to the level of normal fibroblast. The expression of intracellular fibronectin was also increased in WS cells, which was also attenuated by NaHS treatment (Fig. 1D).

The change in autophagy observed in progeria syndromes models [31] may relate to the increase in protein aggregation and insoluble proteins in WS cells. To investigate the presence of autophagy, levels of LC3-I and LC3-II as specific markers of autophagosomes were measured using Western blotting (Fig. 1E)

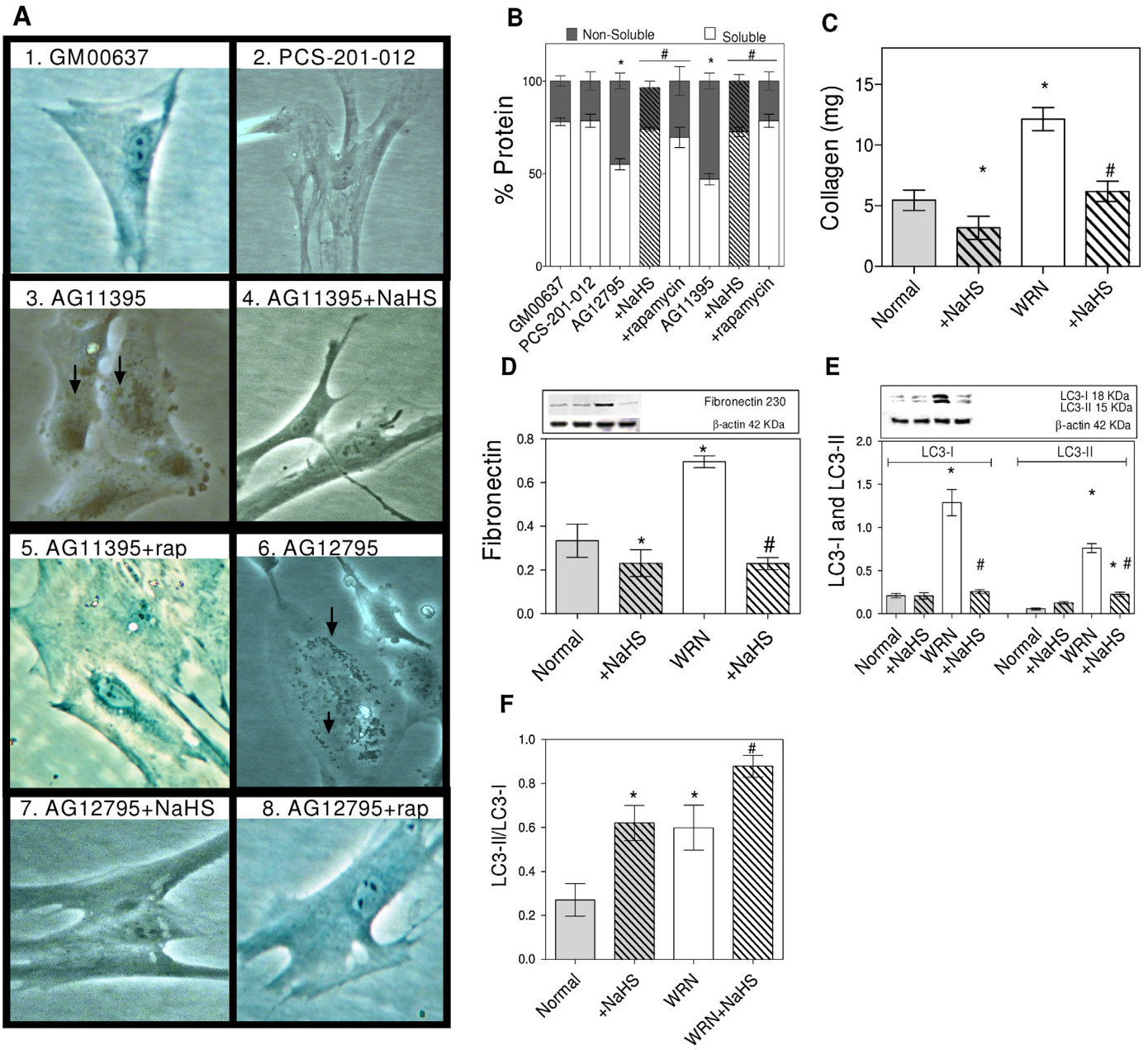

Fig. 1. NaHS treatment restores phenotype, counteracts protein insolubility and normalizes ECM protein synthesis in WS cells. (A) Light microscopic examination demonstrate WS cells (AG11395 and AG12795) to contain cytoplasmic aggregates, which disappear after treatment with NaHS or rapamycin (1 week treatment). WS cells were larger in size with rounder morphology compared to normal or treated cells which were smaller and spindle shaped. (B) WS cells show an increased amount of urea insoluble proteins. Treatment with NaHS normalizes the amount of insoluble protein in WS cells to levels found in normal cells (GM00637, PCS-201-012). (C) and (D) WS cells show excess levels of collagen and fibronectin, which are normalized by NaHS treatment. (E) and (F) WS cells have increased LC3-I and LC3-II levels with higher autophagy levels (LC3-II/LC3-I) and NaHS treatment lowers the levels of LC3-I and LC3-II but increases the levels of autophagy (LC3-II/LC3-I). Data are means ± SD ($n \geq 4$ per group). *: difference to normal cells, #: difference to untreated cells in each group, $P < 0.05$. Western blot expression is normalized to β-actin; lanes of Western blot insets are in the same order as in the *X*-axis.

[32]. Both LC3-I and LC3-II levels were 3–4 times higher in WS cells compared to normal fibroblasts. Thus, we determined the effects of NaHS on the ratio of LC3-II/LC3-I. One week of treatment with NaHS, which had decreased extracellular matrix protein synthesis and intracellular aggregates, lowered LC3-I and LC3-II expression to normal levels but increased autophagy levels as determined by LC3-II/LC3-I ratio in both normal and WS cells.

Together, these data implicate that NaHS and rapamycin treatment normalize protein aggregation and the amount of insoluble proteins. Moreover, NaHS appears to normalize the enhanced production of collagen and fibronectin while increasing the flux through the autophagy pathway.

3.2. mTOR pathway in WS skin fibroblasts and modulation by NaHS

Intracellular aggregates in cells are classically associated with misfolded and aggregated proteins which should normally be degraded. Because of the increase in intracellular aggregates and excess production of collagen and fibronectin, we examined the mTOR pathway, a main controller of protein synthesis [33]. The expression and phosphorylation of mTOR at ser2448 were examined. While total mTOR expression was not increased in WS cells compared to normal, NaHS slightly decreased the expression of this protein in both WS and normal cells (Fig. 2A). mTOR

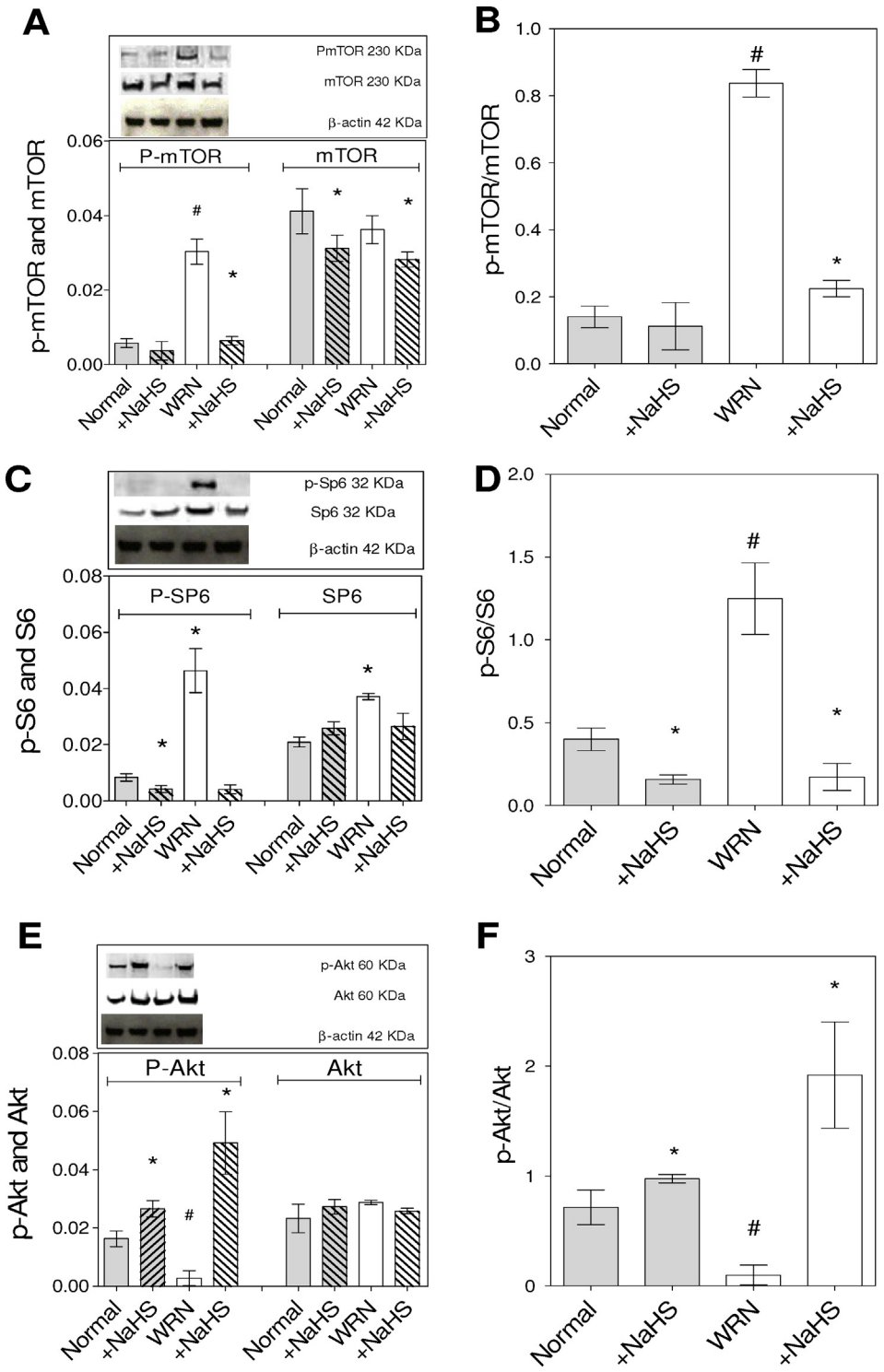

Fig. 2. Changes in mTOR pathway in WS cells are counteracted by NaHS treatment. (A) and (B) WS cells show increased expression and phosphorylation of mTOR at ser2448. NaHS treatment (1 week) decreases the expression and activation of mTOR in both normal cells and WS cells. (C) and (D) WS cells show increased expression and activation of S6 ribosomal protein compared to normal. Treatment of WS cells with NaHS lowered the expression and activation of S6 ribosomal protein. (E) and (F) WS cells show decreased levels of Akt phosphorylation compared to normal cells. Treatment with NaHS increased pAkt in normal and WS cells. Data are means ± SD ($n \geq 3$ per group cell line). *: difference to normal cells, #: difference to untreated cells in each group, $P < 0.05$. Western blot expression is normalized to β-actin; lanes of Western blot insets are in the same order as in the *X*-axis.

phosphorylation, however, was about 4 times higher in WS cells compared to normal, which was normalized by treatment with NaHS (Fig. 2B). Next we examined S6 ribosomal protein (S6) expression, the downstream target of the mTORC1 complex. S6 ribosomal protein showed a higher basal level in WS compared to normal. Further, phospho-S6 ribosomal protein (pS6) was grossly increased in WS cells compared to control (Fig. 2C), which was inhibited by NaHS (Fig. 2D). In addition, WS cells showed down-regulation of the Akt/PKB pathway, as shown by decreased levels of Akt and pAkt compared to normal fibroblasts (Fig. 2E). NaHS treatment modestly increased pAkt levels in control fibroblasts, but strongly increased pAkt levels in WS cells to levels above NaHS

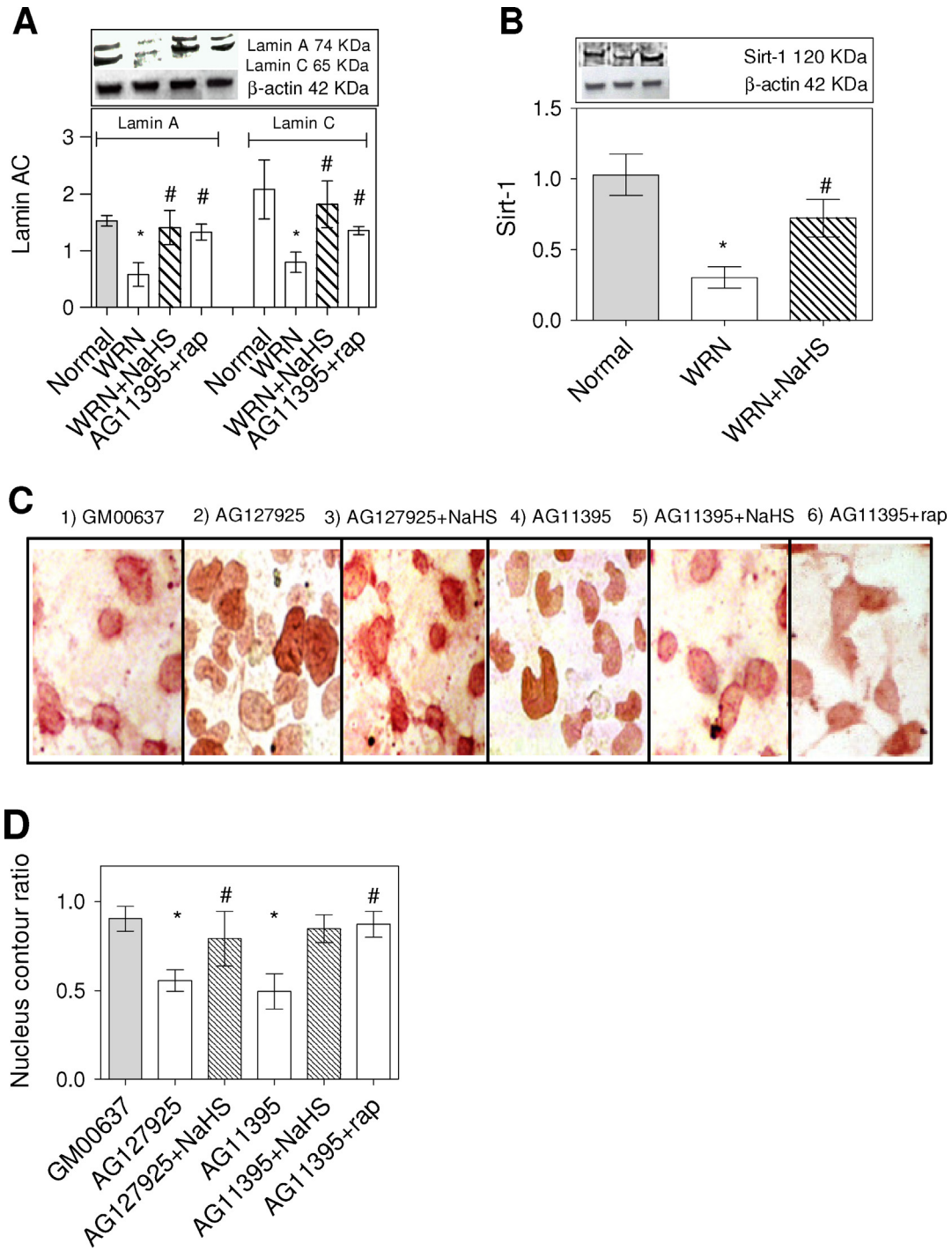

Fig. 3. NaHS treatment normalizes nuclear morphology and SIRT-1 expression. (A) WS cells demonstrate lower lamin A/C expression compared to normal cells, which is restored through NaHS or rapamycin treatment. (B) WS cells show strongly decreased SIRT-1 expression, which is normalized by NaHS treatment. (C) Lamin A/C staining of WS cells shows irregularly shaped nuclei in 50% of the WS cells, which is normalized by treatment with NaHS or rapamycin. Data are means ± SD ($n \geq 3$ per group cell line). (D) Nucleus contour ratio (CR) shows the level of the nuclei roundness. Cells with a CR = 0.7 were considered nonlobulated, and those with a CR < 0.7 were considered lobulated. *: difference to normal cells, #: difference to WS control cells, $P < 0.05$. Western blot expression is normalized to β-actin; lanes of Western blot insets are in the same order as in the *X*-axis.

treated normal fibroblasts (Fig. 2F). Thus, NaHS treatment both inhibited the activated mTOR pathway and strongly induced the Akt survival pathway of WS cells.

3.3. Effects of NaHS on nuclear morphology

As WS fibroblasts are known to exhibit abnormal overall nuclear morphology [34], possibly related to decreased lamin A/C protein levels [35], we examined nuclear morphology and quantified lamin A/C. In accord with senescence, both the expression of lamin A and C was decreased in WS cells (Fig. 3A). Also, WS cells stained for lamin A/C antibody showed nuclei with a distorted shape (Fig. 3C panels 2 and 4), indicating an unstable nucleus morphological structure. Treatment of WS cells with NaHS normalized levels of lamins A and C (Fig. 3A) and restored the abnormal morphological structure of the nucleus (Fig. 3C panels 3 and 5) to normal (Fig. 3C panel 1).

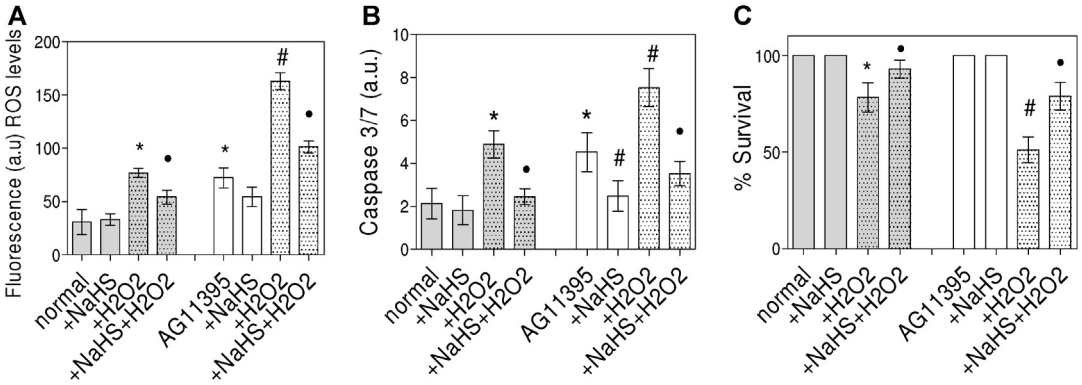

Fig. 4. NaHS induces resistance to ROS damage in cells. (A) WS and normal cells show increased levels of fluorescin fluorescence, as a measure of ROS production, following H_2O_2 treatment, which is attenuated by treatment with NaHS (1 week). (B) WS and normal cells show increased levels of caspase activity following H_2O_2 treatment, which is attenuated by treatment with NaHS. (C) Cell survival following H_2O_2 treatment is decreased in WS cells and normal fibroblast and is attenuated by NaHS. Data are means ± SD ($n \geq 3$ per group cell line). *: difference to normal cells, #: difference to WS untreated cells, •: difference to H_2O_2 treated WS control cells, $P < 0.05$.

Similar effects were observed with rapamycin treatment (Fig. 3C panel 6). Thus, NaHS treatment restores the abnormality in nuclear morphology of WS cells.

In addition to lamins, we examined expression of SIRT1 (sirtuin 1: silent mating type information regulation 2 homolog), a class III histone deacetylase (HDAC) known to promote proliferation and prevent senescence [36]. While levels of SIRT1 were strongly reduced in WS cells, treatment with NaHS completely restored its levels to that of normal cells (Fig. 3B). In normal cells, the contour ratio (CR) remained 0.9 ± 0.1 whereas in WS cells this ratio was lower at 0.5 ± 0.14. Cells with a nucleus CR ≥ 0.7 were considered nonlobulated, and those with a CR < 0.7 were considered lobulated (Fig. 3D). Thus, the WS cells presented in this experiments have lobulated nuclei which is restored to normal through the use of NaHS or rapamycin.

3.4. NaHS treatment induces resistance to senescence and oxidative damage in WS cells

To further substantiate that NaHS treatment restores a normal cellular defense against stress in WS cells, their resistance to oxidative damage was investigated by measuring cell death through oxidative stress. The basal level of oxygen radicals was increased 3-fold in untreated WS cells compared to normal cells (Fig. 4A). Administration of H_2O_2 increased ROS levels of normal cells to the level found in unstimulated WS cells and strongly increased the levels of ROS in WS cells. Treatment with NaHS substantially reduced ROS levels in H_2O_2 treated WS cells and normal fibroblasts to 2/3 of either H_2O_2 treated normal or WS cells (Fig. 4A). In addition, NaHS treatment both lowered caspase 3/7 activity in both H_2O_2 challenged and unchallenged WS cells and H_2O_2 challenged normal fibroblasts (Fig. 4B). Consequently, NaHS treatment increased cell survival in H_2O_2 challenged cells (Fig. 4C).

As WS cells rapidly enter a senescent state [6], we examined the effect of NaHS and rapamycin on premature senescence induced by H_2O_2 treatment by senescence-associated β-galactosidase (SABG) staining. Under basal conditions, about 60% of WS fibroblasts (SV40 nontransfected) stained positive for SABG, while in control this was found to be 17%, which was further increased by treatment with H_2O_2 (Fig. 5). NaHS substantially lowered senescence both in unchallenged WS cells and H_2O_2 treated WS and normal cells. Rapamycin displayed similar effects, although its effectiveness seemed lower compared to NaHS (Fig. 5).

3.5. The H_2S producing endogenous pathway in WS cells

Finally, we investigated the endogenous H_2S pathways known to exert antioxidant activity. Western blot analysis showed that expression of CBS and CSE was significantly reduced in WS cells, and CBS seemed more affected than CSE (Fig. 6A and B). In addition, WS cells displayed lower intracellular levels of thiol groups compared to normal cells. Moreover, thiol levels in WS cells were strongly reduced by challenging with H_2O_2 (Fig. 6C). Finally, NaHS and rapamycin treatment normalized the amount of thiol groups in H_2O_2 challenged WS cells to levels comparable with H_2O_2 challenged normal cells (Fig. 6C). Together, these data show that WS cells show increased vulnerability to oxidative stress and decreased intracellular levels of thiol groups, all of which are counteracted by NaHS and rapamycin treatment.

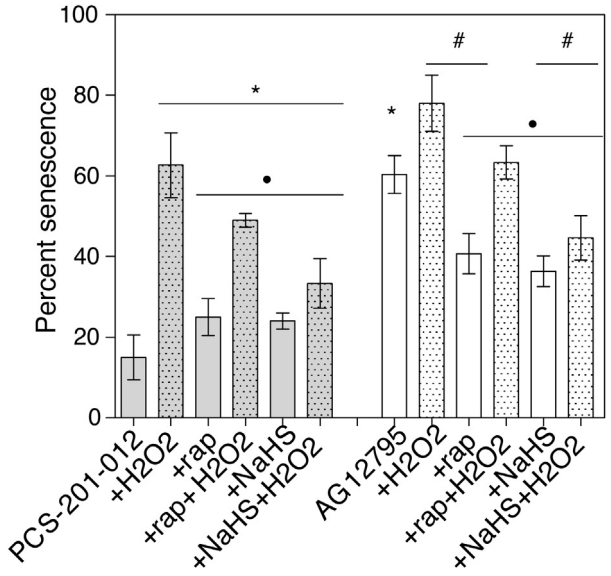

Fig. 5. Percent senescence (SABG) 24 h after subjection to oxidative stress (H_2O_2). SABG staining at pH 6 shows higher levels of senescence in WS cells (AG12795) compared to normal (PCS-201-012). H_2O_2 induced cellular senescence was pharmacologically suppressed by both rapamycin and NaHS treatment. Data are means ± SD ($n \geq 3$ per group cell line). *: difference to normal cells, # difference to WS untreated cells, •: difference to H_2O_2 treated WS and normal cells in each group, $P < 0.05$.

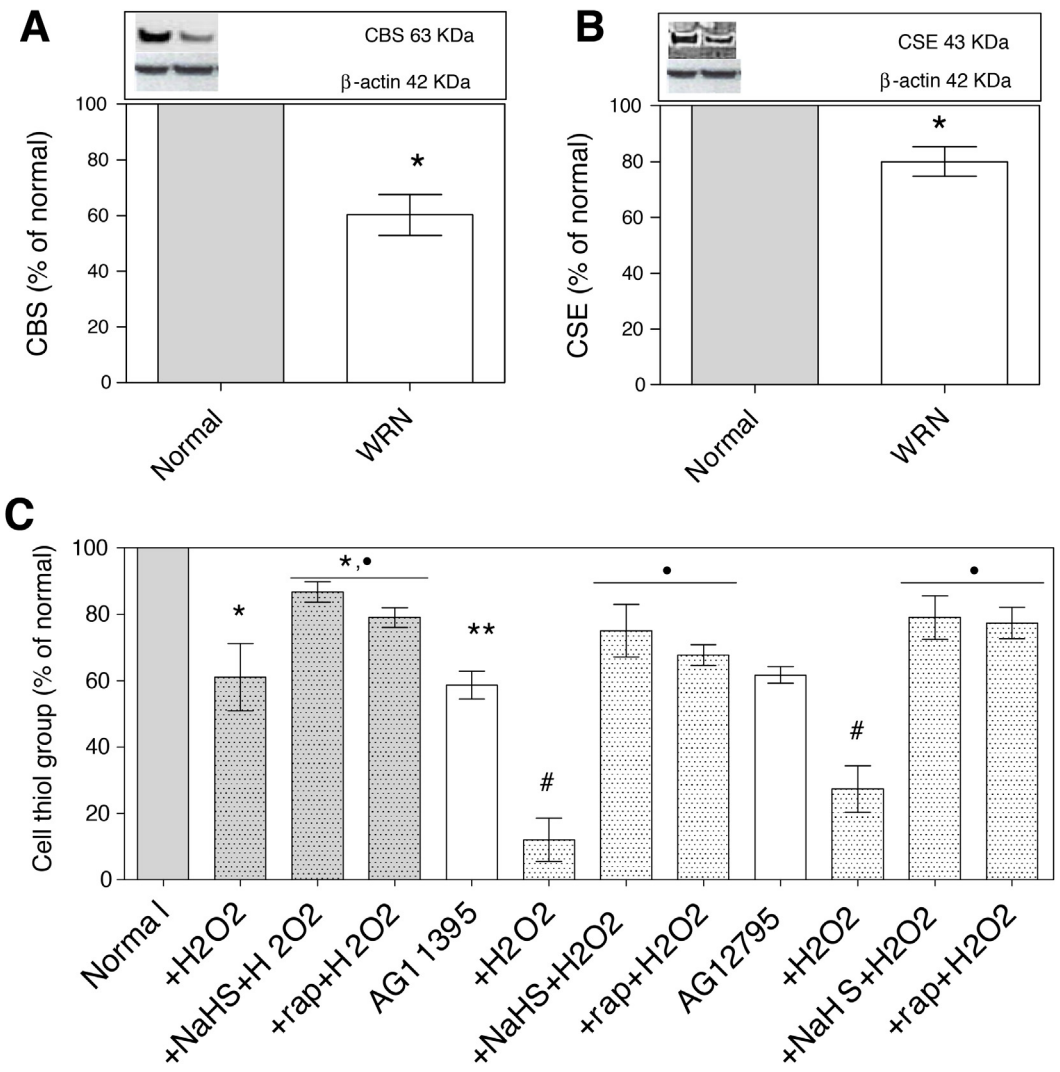

Fig. 6. Expression of H_2S generating enzymes and levels of cellular thiols are reduced in WS cells. (A) and (B) S producing enzymes cystathionine β synthase (CBS) and WS cells show lower expressions of cystathionine γ lyase (CSE) compared to normal. (C) Cellular levels of thiol groups are reduced in WS (AG11395 and AG12795). NaHS and rapamycin treatment increase the levels of free thiol groups in WS cells. H_2O_2 treatment of WS cells strongly decreases the level of free thiol groups, which is attenuated by treatment with NaHS and rapamycin. Data are means ± SD ($n \geq 3$ per group). *: difference to normal cells, #: difference to WS untreated cells, •: difference to H_2O_2 treated WS control cells, $P < 0.05$. Western blot expression is normalized to β-actin; lanes of Western blot insets are in the same order as in the *X*-axis.

4. Conclusion

The current study demonstrates that treatment with NaHS alleviates major changes in cultured WS fibroblasts, essentially restoring their normal morphological phenotype. WS cells were characterized by an increase in intracellular aggregates and abundant production of insoluble proteins, accompanied by a high level of oxidative stress and nuclear dysmorphy, which were alleviated by NaHS treatment. In addition, we found WS cells to display complex changes in protein synthesis and breakdown pathways. On the one hand WS cells display a strong activation of the mTORC1 pathway, as evidenced by the increase in pmTOR and pS6 ribosomal protein levels, which was accompanied by a decrease in pAkt levels most likely caused by a negative feedback from mTORC1 activation. On the other hand, autophagy was induced in WS cells as indicated by strongly increased levels of both LC3-I and LC3-II and an elevated LC3-II/LC3-I ratio of WS cells compared to normal cells. Notably, all these changes in WS cells were attenuated or normalized by 1 week of daily treatment with NaHS. Many of the beneficial effects of NaHS treatment seem to relate to suppression of the mTORC1 pathway, as treatment with the mTOR inhibitor, rapamycin, displayed similar effects as NaHS. Further, NaHS reduced the increased vulnerability to oxidative damage in WS cells, suggesting that the limitation of oxidative damage may represent an additional mechanism of action of NaHS treatment. Indeed, we found the endogenous enzymes involved in the production of H_2S to be downregulated in WS cells, resulting in decreased intracellular levels of thiol groups, likely acting as antioxidants. Taken together, our data implicate that H_2S constitutes a possible treatment option to attenuate excess protein aggregation and oxidative stress in WS fibroblasts.

In contrast to the common notion that the mTORC1 pathway acts as a negative regulator of autophagy, our data suggest that autophagy is activated in WS cells. Indeed, simultaneous activation of both mTORC1 and autophagy has been reported previously in aberrant DNA mismatch repair in 6-thioguanine treated cells accumulating DNA strand breaks [37]. Thus, co-activation of both pathways may result from the severely hampered DNA repair in WS fibroblasts, due to lack of the WRN helicase [20]. Alternatively, co-activation of mTORC1 and autophagy in WS cells may root in a signal that overrides suppression of autophagy by mTORC1. In view of our finding of extensive protein production and protein aggregation in WS cells, one of the likely candidates in WS cells to cause

activation of autophagy may be the unfolded protein response (UPR), which normally results from ER (endoplasmic reticulum) stress and is known to activate autophagy [38]. Moreover, ER stress/UPR activation of autophagy in WS cells may be amplified further by excessive production of ROS in these cells [39]. Taken together, several mechanisms operational in WS, including DNA damage, ER stress and ROS production may explain co-activation of mTORC1 and autophagy in WS fibroblasts, as observed by us.

Our data implicate that protein aggregation, in addition to known factors such as DNA damage [40], constitutes an important mechanism of the phenotypical changes in WS fibroblast. WS cells showed abundant production of insoluble proteins with visible vesicular conformations. It has been proposed that protein aggregation induces growth arrest in cells that are unable to degrade them [41]. Growth suppression is also observed in WRN protein depleted cells [7]. We demonstrate higher levels of extracellular matrix molecules such as collagen and fibronectin produced by WS cells. A novel finding of our study is that the mTORC1 pathway is strongly activated in WS cells, as implied by increased levels of phosphorylated mTOR and S6 ribosomal protein. The marked upregulation of matrix proteins such as collagen and fibronectin in WS cells may well be caused by activation of the mTORC1 complex, which promotes protein synthesis and aggregation [42]. In proliferating cells, growth factors activate cell mass growth, which is balanced by division. When the cell cycle is slower, the activated mTOR could drive the senescent morphology [43]. Moreover, activation of the mTORC1 increases cellular stress [44] which may further explain the protein aggregation we observed in WS cells. In contrast to mTORC1, the mTORC2 pathway seems inhibited as shown by lower pAkt levels [45]. However, the lower pAkt levels in WS cells may also represent the negative feedback of mTORC1 on Akt [46]. Irrespective of its cause, the downregulation of pAkt is likely to lower resistance of WS cells to oxidative stress. In accord with the proposition that activation of mTORC1 contributes to the aberrant phenotype in WS cells, rapamycin treatment decreased the level of insoluble proteins and the amount of aggregates. Also, rapamycin restored the nuclear morphology of WS cell lines, while inhibiting senescence in H_2O_2 challenged cells. Indeed, the activation in the mTORC1 pathway activity in WS fibroblasts is possibly in accord with a recent study in cultured fibroblasts of Hutchinson–Gilford progeria syndrome (HGPS) patients [47], although in HGPS, autophagy is found to be lower compared to normal [48]. In these fibroblasts, treatment with the inhibitor of mTORC1, rapamycin, also restores a normal cellular phenotype and limits protein aggregation. Even though we found autophagy to be higher in WS cells compared to normal, it seems conceivable that rapamycin's beneficial effect in both conditions originates from mTOR inhibition. To date it is still unclear whether the aberrant WRN protein is a prerequisite to induce protein synthesis and protein aggregation in WS cells, but it is known that the reintroduction of WRN protein into WS skin fibroblasts partially protects them from the aging associated accumulation of chromosomal aberrations [8].

Low levels of intracellular thiol groups represents a second new finding in WS cells. In accord with the resulting impairment of anti-oxidant defense, WS cells displayed increased levels of ROS and increased caspase 3/7 activity, and were highly vulnerable to H_2O_2 treatment, as previously demonstrated for UV radiation and cytostatic drugs [49]. Importantly, NaHS treatment attenuated H_2O_2 induced DNA fragmentation in WS cells, suggesting that the beneficial effect of Induction of sulfide bonds around DNA might safeguard the DNA against a high level of oxidization [50], thus, the beneficial effects of NaHS could also result from the attenuation of defects downstream of DNA damage. Low levels of thiol groups in WS fibroblasts seem related to the decreased expression of CBS and CSE, both enzymes involved in the endogenous generation of H_2S [51]. However, the nature of the downregulation of CBS and CSE in cultured WS cells is currently unknown. Likely, the lower thiol levels of WS cells contribute to the excess DNA damage and increase their vulnerability to oxidative stress. Although the depletion of cellular thiol groups has been implicated in aging and the pathogenesis of many diseases [52,53], its contribution to accelerated aging has not been studied. The lower capacity to generate endogenous H_2S in WS possibly also relates to WS patients being prone to atherosclerosis [54], as NaHS treatment attenuates atherosclerosis in ApoE knockout mice [55]. To what extend clinical features of WS depend on reduced thiol formation awaits further studies.

The third major finding is that NaHS treatment restored the phenotype of WS cells. While one may argue that 50 μM of NaHS is out of the physiological range, this concentration proved pharmacologically superior in survival in WS cells compared to lower concentrations. Clearly, NaHS treatment inhibited mTORC1, as evidenced by decreased levels of pmTOR and pS6, while strongly increasing the levels of pAkt. Together, this results in an inhibition of excess production of matrix proteins, and the decrease of protein aggregation. The latter may explain the reduced autophagosome formation in NaHS treated WS cells, which implicate a decreased flux of proteins through the autophagy pathway [56]. Both inhibition of the mTORC1 pathway and increase in pAkt are likely to convey beneficial actions in WS cells. Decrease in mTORC1 maintains cellular quiescence, represses protein production and has been previously observed to extend lifespan in yeast, worms and flies [33]. Increased phosphorylation of Akt is known to promote cell survival [57] and DNA repair [58]. Further, we found an increase in SIRT-1 expression after H_2S treatment. SIRT-1 has been shown to promote autophagy by regulation of the formation of autophagic vacuoles through stimulation of conversion of LC3-I to LC3-II [59,60], negatively regulating mTOR [61], impairing mTORC2/Akt signaling [62] and finally antagonizing senescence [36]. Thus, most likely, SIRT-1 normalization by NaHS reflects an overall higher increase in the levels of soluble proteins, restoring the cellular phenotype.

One of the remaining questions is whether NaHS treatment directly inhibits mTORC1 activation, or whether this results from an upstream action. H_2S actions on cells have been attributed both to its profound scavenging properties [63,64] and to the posttranslational modification of proteins via sulfhydration [65]. In accord with its anti-oxidant effect, NaHS treatment reduced ROS formation both in H_2O_2 challenged and unchallenged WS cells. Previously, the treatment of WS cells with ascorbic acid was shown to limit oxidative damage and extend the lifespan of WS cells [66]. Whether H_2S displays additional effects over ascorbic acid remains unknown, as it is unclear whether the latter restores the phenotype of WS cells. Suppression of metabolism [67] may represent an additional mechanism conveying the beneficial effect of H_2S in WS. Similar to starvation, metabolic suppression by H_2S may inhibit the mTOR pathway [68]. Also, H_2S has the potential to modulate different signaling routes [69,70], affecting multiple kinases including extracellular signal-regulated kinase and Akt. Further, Talaei et al. have shown that H_2S plays an important role in protecting lung structure in hibernating hamster by contributing to a reversible remodeling process [71]. Such effects may add to the protective mechanism(s) of H_2S. Additional effects of H_2S may depend on its action as reductant or its ability to promote sulfhydration of protein cysteine moieties.

In our experiments rapamycin decreased the level of insoluble proteins and the percentage of aggregates visible in WS cells. Also, rapamycin restored the nuclear morphology of in WS cell lines, while inhibiting senescence in H_2O_2 challenged cells. Because of similarity of the beneficial effects of NaHS and rapamycin treatment, these results support NaHS to act beneficially in WS cells through inhibition of mTOR.

In summary, WS fibroblasts used in this research phenotypically appear as highly stressed cells with extensive protein production and aggregation accompanied by nuclear dysmorphy. The purpose of this research was not to find the mechanism of how H_2S restores phenotype in WS fibroblasts but rather the discovery that H_2S administered as NaHS is able to restore a normal morphological phenotype in WS cells. Thus experiments with autophagosome inhibitors to investigate autophagosome maturation were not conducted. Treatment with NaHS normalized the phenotype and proteostasis, most likely through normalization of the mTOR pathway. These findings indicate that restoration of H_2S levels provides an additional pharmacological approach to treatment with rapamycin. Further the potential of NaHS to inhibit mTOR may provide a new strategy against protein aggregation in other progeria symptoms or other types of aggregation prone complications.

Competing interests

No competing interests exist.

Authors' contributions

F.T. and V.V.P. designed the study, managed the literature searches, performed the experiments and performed the statistical analysis, wrote the protocol, and wrote the first and second drafts of the manuscript. R.H.H. managed the design of the study and reviewed the work. All authors read and approved the final manuscript.

References

[1] Thannhauser SJ. Werner's syndrome (progeria of the adult) and Rothmund's syndrome: two types of closely related heredofamilial atrophic dermatoses with juvenile cataracts and endocrine features; a critical study with five new cases. S.J. Tannhauser. Reprinted from Annals of Internal Medicine, 23:559 (1945). Advances in Experimental Medicine and Biology 1985;190:15–56.
[2] Goto M, Miller RW, Ishikawa Y, Sugano H. Excess of rare cancers in Werner syndrome (adult progeria). Cancer Epidemiology, Biomarkers and Prevention 1996;5:239–46.
[3] Yu CE, Oshima J, Fu YH, Wijsman EM, Hisama F, Alisch R, et al. Positional cloning of the Werner's syndrome gene. Science 1996;272:258–62.
[4] Brosh Jr RM, Karow JK, White EJ, Shaw ND, Hickson ID, Bohr VA. Potent inhibition of Werner and bloom helicases by DNA minor groove binding drugs. Nucleic Acids Research 2000;28:2420–30.
[5] Multani AS, Chang S. WRN at telomeres: implications for aging and cancer. Journal of Cell Science 2007;120:713–21.
[6] Dimri GP, Lee X, Basile G, Acosta M, Scott G, Roskelley C, et al. A biomarker that identifies senescent human cells in culture and in aging skin in vivo. Proceedings of the National Academy of Sciences of the United States of America 1995;92:9363–7.
[7] Mao FJ, Sidorova JM, Lauper JM, Emond MJ, Monnat RJ. The human WRN and BLM RecQ helicases differentially regulate cell proliferation and survival after chemotherapeutic DNA damage. Cancer Research 2010;70:6548–55.
[8] Crabbe L, Jauch A, Naeger CM, Holtgreve-Grez H, Karlseder J. Telomere dysfunction as a cause of genomic instability in Werner syndrome. Proceedings of the National Academy of Sciences of the United States of America 2007;104:2205–10.
[9] Chang S, Multani AS, Cabrera NG, Naylor ML, Laud P, Lombard D, et al. Essential role of limiting telomeres in the pathogenesis of Werner syndrome. Nature Genetics 2004;36:877–82.
[10] Lombard DB, Beard C, Johnson B, Marciniak RA, Dausman J, Bronson R, et al. Mutations in the WRN gene in mice accelerate mortality in a p53-null background. Molecular and Cellular Biology 2000;20:3286–91.
[11] Tyedmers J, Mogk A, Bukau B. Cellular strategies for controlling protein aggregation. Nature Reviews Molecular Cell Biology 2010;11:777–88.
[12] Soto C. Unfolding the role of protein misfolding in neurodegenerative diseases. Nature Reviews Neuroscience 2003;4:49–60.
[13] Talaei F. Aberrations in proteostasis orchestrate: the genotypic and phenotypic changes in aging. American Journal of Molecular and Cellular Biology 2012;1:1–16.
[14] Oliver CN, Ahn BW, Moerman EJ, Goldstein S, Stadtman ER. Age-related changes in oxidized proteins. Journal of Biological Chemistry 1987;262:5488–91.
[15] Mirzaei H, Regnier F. Protein: protein aggregation induced by protein oxidation. Journal of Chromatography B: Analytical Technologies in the Biomedical and Life Sciences 2008;873:8–14.
[16] Friguet B. Oxidized protein degradation and repair in ageing and oxidative stress. FEBS Letters 2006;580:2910–6.
[17] Ticozzi N, Ratti A, Silani V. Protein aggregation and defective RNA metabolism as mechanisms for motor neuron damage. CNS and Neurological Disorders Drug Targets 2010;9:285–96.
[18] Lindner AB, Demarez A. Protein aggregation as a paradigm of aging. Biochimica et Biophysica Acta 2009;1790:980–96.
[19] Von Kobbe C, May A, Grandori C, Bohr VA. Werner syndrome cells escape hydrogen peroxide-induced cell proliferation arrest. FASEB Journal 2004;18:1970–2.
[20] Arioshi K, Suzuki K, Goto M, Watanabe M, Kodama S. Increased chromosome instability and accumulation of DNA double-strand breaks in Werner syndrome cells. Journal of Radiation Research 2007;48:219–31.
[21] Faragher RG, Kill IR, Hunter JA, Pope FM, Tannock C, Shall S. The gene responsible for Werner syndrome may be a cell division "counting" gene. Proceedings of the National Academy of Sciences of the United States of America 1993;90:12030–4.
[22] Yang K, Kwon J, Rhim J, Choi J, Kim S, Lee S, et al. Differential expression of extracellular matrix proteins in senescent and young human fibroblasts: a comparative proteomics and microarray study. Molecules and Cells 2011;32:99–106.
[23] Goto M. Hierarchical deterioration of body systems in Werner's syndrome: implications for normal ageing. Mechanisms of Ageing and Development 1997;98:239–54.
[24] Yonezawa D, Sekiguchi F, Miyamoto M, Taniguchi E, Honjo M, Masuko T, et al. A protective role of hydrogen sulfide against oxidative stress in rat gastric mucosal epithelium. Toxicology 2007;241:11–8.
[25] Kimura Y, Kimura H. Hydrogen sulfide protects neurons from oxidative stress. FASEB Journal 2004;18:1165–7.
[26] Lee HJ, Mariappan MM, Feliers D, Cavaglieri RC, Sataranatarajan K, Abboud HE, et al. Hydrogen sulfide inhibits high glucose-induced matrix protein synthesis by activating AMP-activated protein kinase in renal epithelial cells. Journal of Biological Chemistry 2012;287:4451–61.
[27] Foster KG, Fingar DC. Mammalian target of rapamycin (mTOR): conducting the cellular signaling symphony. Journal of Biological Chemistry 2010;285:14071–7.
[28] Dunlop EA, Tee AR. Mammalian target of rapamycin complex 1: signalling inputs, substrates and feedback mechanisms. Cellular Signalling 2009;21:827–35.
[29] Lee DA, Assoku E, Doyle V. A specific quantitative assay for collagen synthesis by cells seeded in collagen-based biomaterials using sirius red F3B precipitation. Journal of Materials Science Materials in Medicine 1998;9:47–51.
[30] Talaei F, Hylkema MN, Bouma HR, Boerema AS, Strijkstra AM, Henning RH, et al. Reversible remodeling of lung tissue during hibernation in the Syrian hamster. Journal of Experimental Biology 2011;214:1276–82.
[31] Marino G, Lopez-Otin C. Autophagy and aging: new lessons from progeroid mice. Autophagy 2008;4:807–9.
[32] Mizushima N, Yamamoto A, Matsui M, Yoshimori T, Ohsumi Y. In vivo analysis of autophagy in response to nutrient starvation using transgenic mice expressing a fluorescent autophagosome marker. Molecular Biology of the Cell 2004;15:1101–11.
[33] Zoncu R, Efeyan A, Sabatini DM. mTOR: from growth signal integration to cancer, diabetes and ageing. Nature Reviews Molecular Cell Biology 2011;12:21–35.
[34] Adelfalk C, Scherthan H, Hirsch-Kauffmann M, Schweiger M. Nuclear deformation characterizes Werner syndrome cells. Cell Biology International 2005;29:1032–7.
[35] Turaga RV, Paquet ER, Sild M, Vignard J, Garand C, Johnson FB, et al. The Werner syndrome protein affects the expression of genes involved in adipogenesis and inflammation in addition to cell cycle and DNA damage responses. Cell Cycle 2009;8:2080–92.
[36] Huang J, Gan Q, Han L, Li J, Zhang H, Sun Y, et al. SIRT1 overexpression antagonizes cellular senescence with activated ERK/S6k1 signaling in human diploid fibroblasts. PLoS ONE 2008;3:e1710.
[37] Zeng X, Kinsella TJ. Mammalian target of rapamycin and S6 kinase 1 positively regulate 6-thioguanine-induced autophagy. Cancer Research 2008;68:2384–90.
[38] Ogata M, Hino S, Saito A, Morikawa K, Kondo S, Kanemoto S, et al. Autophagy is activated for cell survival after endoplasmic reticulum stress. Molecular and Cellular Biology 2006;26:9220–31.
[39] Scherz-Shouval R, Elazar Z. Regulation of autophagy by ROS: physiology and pathology. Trends in Biochemical Sciences 2011;36:30–8.
[40] Avery SV. Molecular targets of oxidative stress. Biochemical Journal 2011;434:201–10.
[41] Arslan MA, Chikina M, Csermely P, Sőti C. Misfolded proteins inhibit proliferation and promote stress-induced death in SV40-transformed mammalian cells. FASEB Journal 2012;26:766–77.
[42] Proud CG. mTORC1 signalling and mRNA translation. Biochemical Society Transactions 2009;37:227–31.
[43] Blagosklonny MV. Progeria, rapamycin and normal aging: recent breakthrough. Aging (Albany NY) 2011;3:685–91.
[44] Reiling JH, Sabatini DM. Increased mTORC1 signaling UPRegulates stress. Molecular Cell 2008;29:533–5.
[45] Bilanges B, Vanhaesebroeck B. A new tool to dissect the function of p70 S6 kinase. Biochemical Journal 2010;431:e1–3.

[46] Hahn-Windgassen A, Nogueira V, Chen CC, Skeen JE, Sonenberg N, Hay N. Akt activates the mammalian target of rapamycin by regulating cellular ATP level and AMPK activity. Journal of Biological Chemistry 2005;280:32081–9.
[47] Cao K, Graziotto JJ, Blair CD, Mazzulli JR, Erdos MR, Krainc D, et al. Rapamycin reverses cellular phenotypes and enhances mutant protein clearance in Hutchinson–Gilford progeria syndrome cells. Science Translational Medicine 2011;3:89ra58.
[48] Graziotto JJ, Cao K, Collins FS, Krainc D. Rapamycin activates autophagy in Hutchinson–Gilford progeria syndrome: implications for normal aging and age-dependent neurodegenerative disorders. Autophagy 2012;8:147–51.
[49] Saito H, Moses RE. Immortalization of Werner syndrome and progeria fibroblasts. Experimental Cell Research 1991;192:373–9.
[50] Kanvah S, Schuster GB. Long-range oxidative damage to DNA: protection of guanines by a nonspecifically bound disulfide. Journal of the American Chemical Society 2002;124:11286–7.
[51] Szabo C. Hydrogen sulphide and its therapeutic potential. Nature Reviews Drug Discovery 2007;6:917–35.
[52] Mungli P, Shetty MS, Tilak P, Anwar N. Total thiols: biomedical importance and their alteration in various disorders. Online Journal of Health and Allied Sciences 2009;8:1–6.
[53] Sivonova M, Tatarkova Z, Durackova Z, Dobrota D, Lehotsky J, Matakova T, et al. Relationship between antioxidant potential and oxidative damage to lipids, proteins and DNA in aged rats. Physiological Research 2007;56: 757–64.
[54] Goto M, Kato Y. Hypercoagulable state indicates an additional risk factor for atherosclerosis in Werner's syndrome. Thrombosis and Haemostasis 1995;73:576–8.
[55] Wang Y, Zhao X, Jin H, Wei H, Li W, Bu D, et al. Role of hydrogen sulfide in the development of atherosclerotic lesions in apolipoprotein E knockout mice. Arteriosclerosis, Thrombosis, and Vascular Biology 2009;29:173–9.
[56] Mizushima N, Yoshimori T. How to interpret LC3 immunoblotting. Autophagy 2007;3:542–5.
[57] Ikeyama S, Kokkonen G, Shack S, Wang XT, Holbrook NJ. Loss in oxidative stress tolerance with aging linked to reduced extracellular signal-regulated kinase and Akt kinase activities. FASEB Journal 2002;16(1):114–6. Epub 2001 Nov 14.
[58] Xu N, Hegarat N, Black EJ, Scott MT, Hochegger H, Gillespie DA. Akt/PKB suppresses DNA damage processing and checkpoint activation in late G2. Journal of Cell Biology 2010;190:297–305.
[59] Salminen A, Kaarniranta K. Regulation of the aging process by autophagy. Trends in Molecular Medicine 2009;15:217–24.
[60] Salminen A, Kaarniranta K. SIRT1: regulation of longevity via autophagy. Cellular Signalling 2009;21:1356–60.
[61] Ghosh HS, McBurney M, Robbins PD. SIRT1 negatively regulates the mammalian target of rapamycin. PLoS ONE 2010;5:e9199.
[62] Wang RH, Kim HS, Xiao C, Xu X, Gavrilova O, Deng CX. Hepatic Sirt1 deficiency in mice impairs mTorc2/Akt signaling and results in hyperglycemia, oxidative damage, and insulin resistance. Journal of Clinical Investigation 2011;121:4477–90.
[63] Geng B, Chang L, Pan C, Qi Y, Zhao J, Pang Y, et al. Endogenous hydrogen sulfide regulation of myocardial injury induced by isoproterenol. Biochemical and Biophysical Research Communications 2004;318:756–63.
[64] Whiteman M, Armstrong JS, Chu SH, Jia-Ling S, Wong BS, Cheung NS, et al. The novel neuromodulator hydrogen sulfide: an endogenous peroxynitrite 'scavenger'? Journal of Neurochemistry 2004;90:765–8.
[65] Mustafa AK, Gadalla MM, Sen N, Kim S, Mu W, Gazi SK, et al. H_2S signals through protein S-sulfhydration. Science Signaling 2009;2:ra72.
[66] Kashino G, Kodama S, Nakayama Y, Suzuki K, Fukase K, Goto M, et al. Relief of oxidative stress by ascorbic acid delays cellular senescence of normal human and Werner syndrome fibroblast cells. Free Radical Biology and Medicine 2003;35:438–43.
[67] Blackstone E, Morrison M, Roth MB. H_2S induces a suspended animation-like state in mice. Science 2005;308:518.
[68] Meijer AJ, Codogno P. Nutrient sensing: TOR's Ragtime. Nature Cell Biology 2008;10:881–3.
[69] Yang C, Yang Z, Zhang M, Dong Q, Wang X, Lan A, et al. Hydrogen sulfide protects against chemical hypoxia-induced cytotoxicity and inflammation in HaCaT cells through inhibition of ROS/NF-kappaB/COX-2 pathway. PLoS ONE 2011;6:e21971.
[70] Tamizhselvi R, Sun J, Koh YH, Bhatia M. Effect of hydrogen sulfide on the phosphatidylinositol 3-kinase-protein kinase B pathway and on caerulein-induced cytokine production in isolated mouse pancreatic acinar cells. Journal of Pharmacology and Experimental Therapeutics 2009;329:1166–77.
[71] Talaei F, Bouma HR, Hylkema MN, Strijkstra AM, Boerema AS, Schmidt M, et al. The role of endogenous H_2S formation in reversible remodeling of lung tissue during hibernation in the Syrian hamster. Journal of Experimental Biology 2012;215:2912–9.